Distribution of Heating in an LVRF Bundle Due to Dysprosium in the Central Element[1]

Kwok Tsang, Adriaan Buijs
Atomic Energy of Canada Limited, 2251 Speakman Drive, Mississauga, ON, Canada L5K 1B2

Abstract

The computer code MCNP was used to establish the effect of adding dysprosium to the central pin of the proposed BRUCE-B CANFLEX® Low-Void-Reactivity Fuel (LVRF) on the heat load of the central pin and the heat balance inside the fuel bundle. The Dy generates heat through radiative capture of thermal neutrons, as well as through beta decay of ^{165}Dy to ^{165}Ho.
We conclude that for fresh fuel, the presence of Dy contributes 26% of the overall heat to the central pin, and 0.5% to the whole fuel bundle. These percentages decrease to 11% and 0.5% at the end-of-life burnup condition. A second, operational quantity is the HPFP ratio (heating-power to fission-power ratio). This ratio is 1.63 for fresh fuel and decreases to 1.19 for fuel at the end-of-life burnup condition.

Keywords: MCNP, CANDU, Void, LVRF, Dysprosium

1. Introduction

The "New Fuel Project", undertaken by Bruce Power is described in Reference 1.

In the early stages of the burnup, the neutron flux in the central pin of Low-Void-Reactivity Fuel (LVRF) is reduced by the addition of dysprosium, which has a large neutron-absorption cross section. As the dysprosium is consumed and the slightly enriched uranium fuel in the outer elements depletes, the neutron flux in the central pin increases. However, the radiative capture of neutrons by Dy, followed by the subsequent emission of photons (and an electron in the decay of ^{165}Dy) contributes to heat generation in the central pin, and, to a much lesser extent, in the outer rings.

This analysis gives an estimate of the contribution of the Dy to the heating of the central pin and the LVRF bundle as a whole. Four burnup states of the fuel are considered in this analysis: *i)* fresh; *ii)* mid-burnup, corresponding to 4091 MWd/Mg(U); *iii)* exit-burnup, corresponding to 7935 MWd/Mg(U), and *iv)* end-of-life burnup, corresponding to 14370 MWd/Mg(U).

The calculations are performed with MCNP Version 5 [2] on a Linux cluster. The isotopic compositions of the irradiated fuel regions are obtained from WIMS-AECL, version 2.5d [3], which is the IST[(2)] version. A new version of this code, WIMS-3.02 provides for a better treatment of resonances (in particular ^{238}U and the Dy isotopes). This leads to a more accurate

[1] This paper was presented at the 9th International Conference on CANDU Fuel, Belleville, Ontario, September 2005
® CANFLEX® is a registered trademark of Atomic Energy of Canada Limited (AECL) and the Korea Atomic Energy Research Institute (KAERI)
[2] IST is the Industry Standard Toolset for the nuclear industry in Canada.

calculation of ^{239}Pu generation within the fuel regions, which is useful for studying the power distribution within the central pin.

2. THE MODEL

The MCNP code version 5 [2], called MCNP5 hereafter, is an increasingly important tool for analyzing CANDU reactors in general and the LVRF fuel in particular. In this analysis, a custom-made library for dysprosium was used to simulate the photons emanating from the neutron-capture reaction properly.

The input file to MCNP5 contains a set of three-dimensional volumes describing the LVRF bundle. However, since the end caps were not modelled explicitly, it is, in fact, a two-dimensional model with reflective boundary conditions at the ends of the bundle. The central pin was subdivided in ten concentric cylinder shells, of which the five outer ones were very thin, in order to capture the fine structure inside the pin, in particular the skin effect. The skin effect is a term to indicate that a particular phenomenon is confined to a very thin layer at the surface of a volume. In this case, it refers to ^{239}Pu production close to the surface.

The isotopic compositions for the irradiated fuel were extracted from the WIMS output file. The WIMS burnup calculation was done with a critical buckling at each step of the irradiation. MCNP5 cannot adjust the buckling; in order to compensate for this, a volume of moderator and a cylindrical shell of natural uranium, to simulate an albedo, surrounded the MCNP5 model of the cell. In each MCNP calculation, the density of the natural uranium was adjusted to obtain a critical cell. This approach was adopted for modelling simplicity; the albedo is expected to preserve the neutronics in the cell of interest better than a reflective boundary (which would not generate a critical cell). The cell-to-cell gamma flux interaction in this representation is an approximation but it has an insignificant impact on the heating calculation in the fuel-element cluster.

3. The Procedure

The heat generated in the LVRF bundle was calculated by a criticality run with MCNP5. This Monte Carlo calculation yielded the heating due to the kinetic energy of the fission products (but not the energy from their decays), as well as due to prompt neutrons and prompt photons. Heating due to radiative capture is included.

An important aspect of the method is that photons are tracked from the point of generation to the point of energy deposition. This distinguishes the method from the WIMS methodology, where all energy associated with a fission event is deposited in the fuel, where the fission occurred.

Tracking of electrons and photons from fission-product and activation-product decays was, however, not performed in the MCNP analyses. Their contributions to the heat balance were obtained by multiplying the relevant Q-values with the corresponding fission or capture rates. The Q-values represent the energy available to electrons and photons, and are essentially equal to the mass difference between an isotope and its decay product. Electrons from these decays do not travel far and were assumed to be absorbed locally. The photons from activation-product decays were accounted for, but not treated separately from the electrons: their energies were also assumed to be deposited locally. The spatial distribution of the decay photons due to fission products was assumed to be identical to that of the prompt photons (excluding the Dy capture photons). This is a reasonable approximation, because the decay photons originate in the same place as the prompt photons and have a comparable energy spectrum.

In the MCNP5 runs, a total of 250 cycles with 50000 neutrons per cycle were generated. This ensured that the relative error on each tally was less than 0.5%. The estimated uncertainty on the k_{eff} value was around 0.2 mk for all runs. The initial source distribution was established in 50 inactive cycles. In each of a number of regions, two tallies were defined: *i)* tally type 4, which tallies the neutron flux integrated over a volume, and *ii)* tally type 6, which tallies the photon energy deposition integrated over a volume. The regions are listed in Table 1; they are the ten subdivisions of the central pin, the inner ring, the middle ring and the outer ring of fuel pins, the coolant in regions corresponding to the fuel, the fuel cladding, the pressure tube, the gap, the calandria tube and the moderator.

The prompt-neutron heating was derived by integrating the product of the volume average flux, the atom concentrations, and the Q values of the total neutron reaction over energy, as shown in the following equation:

$$C\int \varphi(E)R(E)dE,$$

where $\varphi(E)$ is the energy-dependent fluence (particles/cm^2), $R(E)$ is the product of the Q value and the associated total cross section (see Reference 2, p. 3-93), and C is the atom density.

In this MCNP analysis, the quantities used are the total neutron cross section and the average heat deposit. The neutron-induced heating was obtained by multiplying the fluence by the total neutron cross section and by the average heat deposit in MeV/collision.

4. Results

4.1. Regional Power Distribution in the Bundle

The main results are presented in Tables 1 to 4, for fresh fuel, fuel at mid-burnup, fuel at exit-burnup, and end-of-life fuel, respectively. They are based on the WIMS-AECL, version 2.5d, fuel compositions. The tables show the fraction of the total bundle power deposited in each of the regions listed. For simplicity, a bundle generating 100 kW in the lattice cell was assumed. The total adds up to 100% as expected (note that this only shows that the calculation is internally consistent; it does not prove that all physics processes are properly accounted for). The total excludes the columns labelled ‘Dy only’, since the Dy-capture photons are already included in the contribution from the prompt photons as listed in the previous column.

Table 1: Relative Power Distribution Per Region and Per Process; Fresh Fuel

	Total	Prompt neutrons		Prompt photons				Fission product decay				Activation product decay			
				Incl. Dy		Dy only		gamma		beta		U239 + Dy165		Dy165 only	
Region	(kW)	(kW)	% of total	(kW)	% of total	(kW)	% of total	(kW)	% of total	(kW)	% of total	(kW)	% of total	(kW)	% of total
CP R1 coarse mesh	0.12	0.06	48.9	0.045	39.4	0.031	27.1	0.008	6.5	0.0025	2.2	0.0035	3.0	0.0030	2.6
CP R2 "	0.13	0.06	51.0	0.047	37.4	0.032	25.8	0.008	6.2	0.0026	2.1	0.0043	3.4	0.0037	3.0
CP R3 "	0.14	0.07	53.2	0.049	35.0	0.033	24.1	0.008	5.8	0.0030	2.2	0.0052	3.8	0.0046	3.3
CP R4 "	0.16	0.09	56.2	0.050	32.1	0.034	22.0	0.008	5.3	0.0035	2.2	0.0065	4.2	0.0058	3.8
CP R5 "	0.18	0.11	60.0	0.049	28.1	0.033	18.8	0.009	4.9	0.0040	2.3	0.0083	4.7	0.0075	4.3
CP R6 fine mesh	0.021	0.013	62.7	0.0053	25.0	0.0034	16.3	0.0010	4.6	0.00056	2.6	0.0011	5.0	0.0010	4.6
CP R7 "	0.022	0.014	63.4	0.0052	24.2	0.0034	15.6	0.0010	4.6	0.00058	2.7	0.0011	5.2	0.0010	4.7
CP R8 "	0.022	0.014	64.3	0.0051	23.3	0.0033	14.8	0.0010	4.5	0.00058	2.6	0.0012	5.3	0.0011	4.8
CP R9 "	0.023	0.015	65.1	0.0050	22.2	0.0031	13.9	0.0010	4.4	0.00062	2.7	0.0012	5.5	0.0011	5.0
CP R10 "	0.023	0.015	66.3	0.0049	21.1	0.0030	12.9	0.0010	4.4	0.00060	2.6	0.0013	5.6	0.0012	5.0
Total Central Pin	**0.82**	**0.46**	**55.8**	**0.27**	**32.4**	**0.18**	**22.0**	**0.045**	**5.5**	**0.019**	**2.3**	**0.034**	**4.10**	**0.030**	**3.7**
Fuel Inner Ring	15.07	13.11	87.0	0.96	6.4	0.15	1.0	0.43	2.9	0.51	3.4	0.05	0.34		
Fuel Middle ring	26.84	23.82	88.8	1.33	4.9	0.06	0.2	0.67	2.5	0.93	3.5	0.09	0.32		
Fuel Outer ring	52.39	47.42	90.5	1.94	3.7	0.04	0.1	1.01	1.9	1.84	3.5	0.17	0.32		
Total Fuel	**95.11**	**84.81**	**89.2**	**4.50**	**4.7**	**0.42**	**0.44**	**2.17**	**2.3**	**3.300**	**3.5**	**0.34**	**0.36**	**0.0040**	**0.0042**
Clad Central Pin	0.01	0.000	0.8	0.01	79.6	0.01	42.7	0.00	19.6						
Clad Inner Ring	0.07	0.001	1.2	0.05	69.0	0.01	13.1	0.02	29.8						
Clad Middle Ring	0.10	0.001	1.3	0.06	65.7	0.00	3.7	0.03	33.0						
Clad Outer Ring	0.13	0.002	1.4	0.09	65.0	0.00	1.9	0.04	33.6						
Total Clad	**0.31**	**0.004**	**1.3**	**0.21**	**66.7**	**0.02**	**6.6**	**0.10**	**32.0**						
Coolant Central Pin	0.02	0.01	60.1	0.00	30.3	0.00	12.1	0.00	9.7						
Coolant Inner Ring	0.11	0.07	64.0	0.03	25.0	0.01	4.5	0.01	10.9						
Coolant Middle Ring	0.17	0.11	64.4	0.04	23.7	0.00	1.2	0.02	11.9						
Coolant Outer Ring	0.25	0.16	63.5	0.06	24.1	0.00	0.6	0.03	12.5						
Total Coolant	**0.55**	**0.35**	**63.8**	**0.13**	**24.3**	**0.01**	**1.9**	**0.07**	**11.9**						
Pressure tube	0.52	0.01	1.2	0.34	65.0	0.01	1.5	0.17	33.8						
Gap	0.00	0.00	18.5	0.00	53.7	0.00	1.3	0.00	27.9						
Calandria tube	0.20	0.00	1.7	0.13	64.7	0.00	1.5	0.07	33.6						
Moderator	3.31	1.44	43.6	1.23	37.0	0.02	0.5	0.64	19.4						
Total	**4.02**	**1.45**	**36.1**	**1.69**	**41.9**	**0.03**	**0.68**	**0.88**	**21.9**						
Grand Total	**100.00**	**86.62**	**86.6**	**6.52**	**6.5**	**0.48**	**0.48**	**3.21**	**3.21**	**3.30**	**3.30**	**0.34**	**0.34**	**0.0040**	**0.0040**

Table 2: Relative Power Distribution Per Region and Per Process; Irradiated Fuel at mid-burnup (4091 MWd/MG(U))

	Total	**Prompt neutrons**		**Prompt photons**				**Fission product decay**				**Activation product decay**			
				Incl. Dy		**Dy only**		**gamma**		**beta**		**U239 + Dy165**		**Dy165 only**	
Region	(kW)	(kW)	% of total	(kW)	% of total	(kW)	% of total	(kW)	% of total	(kW)	% of total	(kW)	% of total	(kW)	% of total
CP R1 coarse mesh	0.14	0.08	57.8	0.047	32.4	0.030	21.1	0.007	5.1	0.0033	2.3	0.0035	2.4	0.0029	2.0
CP R2 "	0.16	0.09	60.0	0.047	30.4	0.031	19.7	0.008	4.8	0.0034	2.2	0.0040	2.6	0.0034	2.2
CP R3 "	0.17	0.11	61.9	0.049	28.4	0.031	18.3	0.008	4.5	0.0040	2.3	0.0047	2.8	0.0041	2.4
CP R4 "	0.19	0.12	64.1	0.049	26.3	0.032	16.9	0.008	4.2	0.0044	2.3	0.0056	3.0	0.0049	2.6
CP R5 "	0.21	0.14	67.1	0.049	23.2	0.030	14.5	0.008	3.9	0.0051	2.4	0.0068	3.3	0.0060	2.9
CP R6 fine mesh	0.025	0.017	68.9	0.0052	21.0	0.0032	12.7	0.0009	3.7	0.00070	2.8	0.0009	3.5	0.0008	3.1
CP R7 "	0.025	0.018	69.6	0.0052	20.5	0.0031	12.3	0.0009	3.7	0.00069	2.7	0.0009	3.5	0.0008	3.1
CP R8 "	0.026	0.018	70.2	0.0051	20.0	0.0030	11.7	0.0009	3.7	0.00066	2.6	0.0009	3.6	0.0008	3.1
CP R9 "	0.026	0.018	70.8	0.0050	19.3	0.0029	11.1	0.0010	3.7	0.00067	2.6	0.0010	3.7	0.0008	3.2
CP R10 "	0.027	0.019	71.7	0.0049	18.2	0.0027	10.2	0.0010	3.6	0.00071	2.7	0.0010	3.9	0.0009	3.4
Total Central Pin	**1.00**	**0.63**	**63.6**	**0.27**	**26.7**	**0.17**	**17.0**	**0.044**	**4.4**	**0.024**	**2.4**	**0.029**	**3.0**	**0.025**	**2.6**
Fuel Inner Ring	15.77	13.78	87.4	1.03	6.5	0.14	0.9	0.40	2.5	0.50	3.2	0.05	0.3		
Fuel Middle ring	27.18	24.17	88.9	1.43	5.3	0.06	0.2	0.61	2.3	0.87	3.2	0.09	0.3		
Fuel Outer ring	50.92	46.10	90.5	2.09	4.1	0.04	0.1	0.92	1.8	1.64	3.2	0.18	0.3		
Total Fuel	**94.86**	**84.69**	**89.3**	**4.81**	**5.1**	**0.41**	**0.43**	**1.97**	**2.1**	**3.038**	**3.2**	**0.35**	**0.37**	**0.025**	**0.027**
Clad Central Pin	0.01	0.000	0.9	0.01	80.5	0.01	39.0	0.00	18.6						
Clad Inner Ring	0.07	0.001	1.2	0.05	71.8	0.01	11.8	0.02	26.9						
Clad Middle Ring	0.10	0.001	1.3	0.07	69.2	0.00	3.5	0.03	29.5						
Clad Outer Ring	0.14	0.002	1.4	0.09	68.6	0.00	1.7	0.04	30.0						
Total Clad	**0.32**	**0.004**	**1.3**	**0.22**	**70.0**	**0.02**	**5.9**	**0.09**	**28.7**						
Coolant Central Pin	0.02	0.01	60.9	0.01	30.4	0.00	10.9	0.00	8.7						
Coolant Inner Ring	0.12	0.08	64.7	0.03	25.6	0.00	4.0	0.01	9.7						
Coolant Middle Ring	0.18	0.12	64.8	0.04	24.7	0.00	1.1	0.02	10.6						
Coolant Outer Ring	0.26	0.17	63.8	0.07	25.2	0.00	0.6	0.03	11.0						
Total Coolant	**0.58**	**0.37**	**64.2**	**0.15**	**25.3**	**0.01**	**1.7**	**0.06**	**10.6**						
Pressure tube	0.53	0.01	1.2	0.37	68.6	0.01	1.4	0.16	30.2						
Gap	0.00	0.00	18.6	0.00	56.5	0.00	1.0	0.00	24.9						
Calandria tube	0.20	0.00	1.7	0.14	68.2	0.00	1.1	0.06	30.1						
Moderator	3.51	1.52	43.4	1.38	39.2	0.02	0.5	0.61	17.4						
Total	**4.24**	**1.53**	**36.1**	**1.88**	**44.3**	**0.03**	**0.63**	**0.83**	**19.6**						
Grand Total	**100.00**	**86.60**	**86.6**	**7.06**	**7.1**	**0.46**	**0.46**	**2.96**	**2.96**	**3.04**	**3.04**	**0.35**	**0.35**	**0.0255**	**0.0255**

Table 3: Relative Power Distribution Per Region and Per Process; Irradiated Fuel at exit burnup (7935 MWd/MG(U))

	Total	Prompt neutrons		Prompt photons				Fission product decay				Activation product decay			
				Incl. Dy		Dy only		gamma		beta		U239 + Dy165		Dy165 only	
Region	(kW)	(kW)	% of total	(kW)	% of total	(kW)	% of total	(kW)	% of total	(kW)	% of total	(kW)	% of total	(kW)	% of total
CP R1 coarse mesh	0.19	0.12	64.3	0.051	27.4	0.032	17.1	0.008	4.1	0.0044	2.4	0.0036	1.9	0.0029	1.6
CP R2 "	0.20	0.13	65.8	0.052	26.0	0.032	16.2	0.008	3.9	0.0046	2.3	0.0039	2.0	0.0032	1.6
CP R3 "	0.21	0.14	67.4	0.052	24.4	0.032	15.1	0.008	3.7	0.0053	2.5	0.0045	2.1	0.0037	1.7
CP R4 "	0.23	0.16	69.3	0.052	22.5	0.032	13.7	0.008	3.5	0.0059	2.5	0.0051	2.2	0.0043	1.8
CP R5 "	0.25	0.18	71.7	0.051	20.2	0.030	11.9	0.008	3.3	0.0064	2.5	0.0059	2.3	0.0050	2.0
CP R6 fine mesh	0.030	0.022	73.4	0.0055	18.4	0.0031	10.5	0.0009	3.2	0.00075	2.5	0.0007	2.5	0.0006	2.1
CP R7 "	0.030	0.022	73.7	0.0054	17.9	0.0030	10.1	0.0009	3.1	0.00083	2.8	0.0008	2.5	0.0006	2.1
CP R8 "	0.030	0.023	74.1	0.0053	17.5	0.0029	9.6	0.0009	3.1	0.00083	2.7	0.0008	2.5	0.0007	2.2
CP R9 "	0.031	0.023	74.8	0.0052	16.9	0.0028	9.2	0.0010	3.1	0.00079	2.6	0.0008	2.6	0.0006	2.1
CP R10 "	0.032	0.024	75.4	0.0051	16.1	0.0027	8.6	0.0009	3.0	0.00090	2.9	0.0008	2.6	0.0007	2.1
Total Central Pin	**1.24**	**0.85**	**68.7**	**0.28**	**23.0**	**0.17**	**14.0**	**0.044**	**3.6**	**0.031**	**2.5**	**0.027**	**2.2**	**0.022**	**1.8**
Fuel Inner Ring	16.50	14.44	87.5	1.11	6.7	0.14	0.8	0.39	2.3	0.51	3.1	0.06	0.3		
Fuel Middle ring	27.42	24.35	88.8	1.53	5.6	0.06	0.2	0.58	2.1	0.85	3.1	0.10	0.4		
Fuel Outer ring	49.44	44.64	90.3	2.22	4.5	0.04	0.1	0.86	1.7	1.52	3.1	0.19	0.4		
Total Fuel	**94.59**	**84.28**	**89.1**	**5.15**	**5.4**	**0.41**	**0.43**	**1.88**	**2.0**	**2.91**	**3.1**	**0.37**	**0.40**	**0.022**	**0.024**
Clad Central Pin	0.01	0.000	0.9	0.01	81.5	0.00	36.9	0.00	17.7						
Clad Inner Ring	0.07	0.001	1.2	0.05	73.9	0.01	11.3	0.02	24.8						
Clad Middle Ring	0.10	0.001	1.3	0.07	71.6	0.00	3.5	0.03	27.0						
Clad Outer Ring	0.14	0.002	1.4	0.10	71.1	0.00	1.8	0.04	27.5						
Total Clad	**0.33**	**0.004**	**1.3**	**0.24**	**72.3**	**0.02**	**5.8**	**0.09**	**26.3**						
Coolant Central Pin	0.02	0.01	60.8	0.01	31.0	0.00	10.4	0.00	8.2						
Coolant Inner Ring	0.12	0.08	64.4	0.03	26.6	0.00	3.9	0.01	9.0						
Coolant Middle Ring	0.19	0.12	64.5	0.05	25.8	0.00	1.2	0.02	9.7						
Coolant Outer Ring	0.27	0.17	63.3	0.07	26.4	0.00	0.6	0.03	10.2						
Total Coolant	**0.60**	**0.38**	**63.8**	**0.16**	**26.4**	**0.01**	**1.8**	**0.06**	**9.8**						
Pressure tube	0.56	0.01	1.2	0.40	71.1	0.01	1.4	0.15	27.6						
Gap	0.00	0.00	18.2	0.00	58.9	0.00	1.1	0.00	22.9						
Calandria tube	0.21	0.00	1.7	0.15	70.7	0.00	1.1	0.06	27.6						
Moderator	3.71	1.59	42.7	1.53	41.2	0.02	0.5	0.60	16.1						
Total	**4.48**	**1.60**	**35.6**	**2.08**	**46.3**	**0.03**	**0.67**	**0.81**	**18.1**						
Grand Total	**100.00**	**86.26**	**86.3**	**7.62**	**7.6**	**0.47**	**0.47**	**2.83**	**2.83**	**2.91**	**2.91**	**0.37**	**0.37**	**0.022**	**0.022**

Table 4: Relative Power Distribution Per Region and Per Process; Irradiated Fuel at end-of-life burnup (14370 MWd/MG(U))

	Total	Prompt neutrons		Prompt photons				Fission product decay				Activation product decay			
				Incl. Dy		Dy only		gamma		beta		U239 + Dy165		Dy165 only	
Region	(kW)	(kW)	% of total	(kW)	% of total	(kW)	% of total	(kW)	% of total	(kW)	% of total	(kW)	% of total	(kW)	% of total
CP R1 coarse mesh	0.26	0.19	71.9	0.055	21.4	0.032	12.5	0.008	3.0	0.0068	2.6	0.0030	1.2	0.0021	0.8
CP R2 "	0.27	0.20	73.0	0.055	20.3	0.032	11.7	0.008	2.9	0.0069	2.5	0.0032	1.2	0.0023	0.9
CP R3 "	0.29	0.21	74.1	0.055	19.2	0.031	10.9	0.008	2.8	0.0076	2.7	0.0035	1.2	0.0026	0.9
CP R4 "	0.30	0.23	75.5	0.054	18.0	0.030	9.9	0.008	2.7	0.0077	2.5	0.0038	1.3	0.0028	0.9
CP R5 "	0.32	0.25	77.0	0.052	16.4	0.028	8.7	0.008	2.6	0.0086	2.7	0.0042	1.3	0.0031	1.0
CP R6 fine mesh	0.037	0.029	78.2	0.0056	15.3	0.0028	7.7	0.0009	2.5	0.00098	2.7	0.0005	1.3	0.0004	1.0
CP R7 "	0.037	0.029	78.5	0.0055	14.9	0.0027	7.4	0.0009	2.5	0.00100	2.7	0.0005	1.4	0.0004	1.0
CP R8 "	0.038	0.030	78.8	0.0055	14.5	0.0027	7.1	0.0009	2.5	0.00103	2.7	0.0005	1.4	0.0004	1.0
CP R9 "	0.038	0.030	79.3	0.0054	14.2	0.0026	6.8	0.0009	2.5	0.00101	2.7	0.0005	1.4	0.0004	1.0
CP R10 "	0.038	0.030	79.7	0.0052	13.7	0.0024	6.4	0.0009	2.5	0.00098	2.6	0.0006	1.5	0.0004	1.1
Total Central Pin	**1.62**	**1.22**	**74.9**	**0.30**	**18.4**	**0.17**	**10.2**	**0.045**	**2.8**	**0.043**	**2.6**	**0.020**	**1.2**	**0.015**	**0.91**
Fuel Inner Ring	17.02	14.87	87.4	1.21	7.1	0.13	0.8	0.36	2.1	0.51	3.0	0.06	0.4		
Fuel Middle ring	27.13	24.01	88.5	1.67	6.1	0.05	0.2	0.54	2.0	0.80	3.0	0.11	0.4		
Fuel Outer ring	48.38	43.52	90.0	2.42	5.0	0.04	0.1	0.80	1.7	1.42	2.9	0.22	0.4		
Total Fuel	**94.16**	**83.62**	**88.8**	**5.60**	**5.9**	**0.38**	**0.41**	**1.76**	**1.9**	**2.77**	**2.9**	**0.41**	**0.44**	**0.015**	**0.016**
Clad Central Pin	0.01	0.000	0.9	0.01	82.3	0.00	32.4	0.00	16.8						
Clad Inner Ring	0.08	0.001	1.3	0.06	76.3	0.01	9.8	0.02	22.4						
Clad Middle Ring	0.11	0.001	1.3	0.08	74.5	0.00	2.9	0.03	24.1						
Clad Outer Ring	0.15	0.002	1.4	0.11	74.0	0.00	1.3	0.04	24.5						
Total Clad	**0.35**	**0.005**	**1.4**	**0.26**	**75.0**	**0.02**	**4.9**	**0.08**	**23.6**						
Coolant Central Pin	0.02	0.01	60.6	0.01	31.8	0.00	9.1	0.00	7.7						
Coolant Inner Ring	0.13	0.08	63.9	0.04	27.9	0.00	3.4	0.01	8.2						
Coolant Middle Ring	0.19	0.12	63.7	0.05	27.4	0.00	1.0	0.02	8.9						
Coolant Outer Ring	0.28	0.17	62.3	0.08	28.3	0.00	0.5	0.03	9.4						
Total Coolant	**0.62**	**0.39**	**63.0**	**0.17**	**28.1**	**0.01**	**1.5**	**0.06**	**8.9**						
Pressure tube	0.60	0.01	1.2	0.45	74.2	0.01	1.3	0.15	24.6						
Gap	0.00	0.00	17.3	0.00	62.1	0.00	1.1	0.00	20.6						
Calandria tube	0.24	0.00	1.7	0.17	73.8	0.00	1.1	0.06	24.5						
Moderator	4.04	1.66	41.1	1.78	44.2	0.02	0.5	0.59	14.7						
Total	**4.87**	**1.67**	**34.3**	**2.40**	**49.3**	**0.03**	**0.62**	**0.80**	**16.4**						
Grand Total	**100.00**	**85.69**	**85.7**	**8.44**	**8.4**	**0.44**	**0.44**	**2.69**	**2.69**	**2.77**	**2.77**	**0.41**	**0.41**	**0.015**	**0.015**

The column labelled 'total' represents the sum of the various energy components per region. These components are

1. The heat from prompt neutrons. This includes the heat from the kinetic energy of the fission products, as well as the heat from neutron interactions in the material of the lattice cell.
2. The heat from prompt photons. This includes the heat from photons emanating from the fission as well as photons from radiative neutron captures. The latter also include the radiative-capture photons in dysprosium. In order to assess the contribution from Dy, a separate MCNP5 run was performed with Dy libraries that did not contain photon data; the difference between the two is the contribution from Dy alone and is listed in the column labelled 'Dy only'.
3. The heat from fission-product gamma and beta decays. These were derived directly from the fission rates of the fissionable isotopes in the fuel (^{235}U and ^{238}U in fresh fuel; ^{235}U, ^{238}U, ^{239}Pu, and ^{241}Pu in irradiated fuel) and the corresponding Q-values. Note that the energy from capture events is included in the prompt photon column. As mentioned before, the electrons and photons from these decays are not tracked through the cell. The photons are distributed spatially according to the prompt-photon distribution (excluding the photons from Dy-captures).
4. The heat from activation-product gamma and beta decays. These were derived directly from the capture rates of ^{164}Dy and ^{238}U in the fuel and the corresponding Q-values. No distinction was made between the electron and the photon energy: both were deposited locally.

Each column is followed by a column showing the percentage of the contribution to the total in that region as shown in the second column.

The regions CP R1 to R10 represent the subdivisions of the central pin. The thickness of the five outer cylindrical shells is much less than that of the five inner shells, so that the power in those shells is correspondingly smaller. Figure 1 shows the power density across the central pin; it shows a rise towards the edge of the pin, which, according to WIMS-2.5d, becomes more pronounced with increasing burnup. The figure also includes the results based on the WIMS-3.02 fuel compositions. It can be seen that the power profile is much more sharply peaked at the edge due to more accurate modelling of Pu239 build-up than in the case of the WIMS-AECL-based calculation. Note, however, the fine structure of the power density within an element is not directly related to the overall gamma heating effect.

4.2. Heat-Power to Fission-Power Ratio (HPFPR)

In WIMS calculations, all energy associated with a fission event is deemed deposited at the location of the fission. In reality this is not so, as some energy (e.g., photon energy) may leak in or out of the fuel. This effect is especially large in LVRF, where Dy is concentrated in a single pin. It then becomes important to correct the energy distribution calculated with WIMS. We can do this by applying the heat-power to fission-power ratios (HPFPR) to the pin powers of WIMS. The fission power is defined here as the fission rate calculated by MCNP5 in each fuel region multiplied by the fission energy used by WIMS. The heat power is the sum of all energy deposited in each fuel region, according to MCNP (for the components generated by MCNP, and spatially distributed according to MCNP for those not generated in MCNP), as shown in Tables 1 to 4. The HPFPR is the ratio of the heat power over the fission power as given by the following equation:

$$\text{HPFPR} = \frac{(Prompt\ n) + (Prompt\ \gamma) + (FP\ \gamma) + (FP\ \beta) + (Activation\ \beta) + (Activation\ \gamma)}{\sum_i (fission\ rates)_i \times Q_i},$$

Where i = fissile nuclide i.

The HPFPRs for the four fuel regions are listed in Table 5, as a function of irradiation. They are based on the isotope compositions calculated by WIMS-AECL.

The values for the central pin are higher than 1, meaning that the inflow of energy per fission is higher than the outflow. The ratios for the other fuel regions are closer to one. The last column shows the HPFPR for the whole bundle. It is lower than one, reflecting the loss of power to the coolant, the moderator and the pressure and calandria tubes. Table 6 shows the same numbers, but divided by the bundle HPFPR. In this way, the numbers have been normalized such that the fission-power weighted average is equal to 1. This is done to ensure that the total bundle power is the same for all burnup values.

Table 5: Heat-Power to Fission-Power Ratios

	Burnup (MWD/Mg(U)	**Central Pin**	**Inner Ring**	**Middle Ring**	**Outer Ring**	**Whole Bundle**
	WIMS-2.5d					
Fresh fuel	0	1.534	0.966	0.948	0.925	0.941
Mid-burnup	4091	1.377	0.969	0.950	0.932	0.946
Exit-burnup	7935	1.253	0.965	0.951	0.934	0.947
End-of-life burnup	14370	1.132	0.970	0.960	0.942	0.955
	WIMS-3.02					
Mid-burnup	4091	1.344	0.967	0.951	0.932	0.946
Exit-burnup	7936	1.220	0.966	0.954	0.934	0.948
End-of-life burnup	14373	1.119	0.972	0.958	0.942	0.955

Table 6: Heat-Power to Fission-Power Ratio, normalised to the bundle HPFPR

	Burnup (MWD/Mg(U)	**Central Pin**	**Inner Ring**	**Middle Ring**	**Outer Ring**
	WIMS-AECL				
Fresh fuel	0	1.630	1.026	1.007	0.983
Mid-burnup	4091	1.455	1.024	1.004	0.985
Exit-burnup	7935	1.323	1.019	1.004	0.986
End-of-life burnup	14370	1.186	1.016	1.005	0.987
	WIMS-3.02				
Mid-burnup	4091	1.420	1.022	1.005	0.985
Exit-burnup	7936	1.286	1.019	1.006	0.985
End-of-life burnup	14373	1.171	1.018	1.003	0.987

Tables 5 and 6 also show the HPFPRs based on isotopic compositions calculated by WIMS version 3.02. The results are very similar to the WIMS-AECL results, except for the central element, where the WIMS-3.02 version predicts a slightly lower ratio. This is due to the fact that WIMS-3.02 predicts an increased power production at the edge of the central element, due to a build-up of ^{239}Pu, combined with a depletion of Dy, near the edge (see Figure 1).

Figure 1 Power Density Distribution within the Central Pin.
The solid lines are based on WIMS-AECL; the dashed lines are based on WIMS-3.02

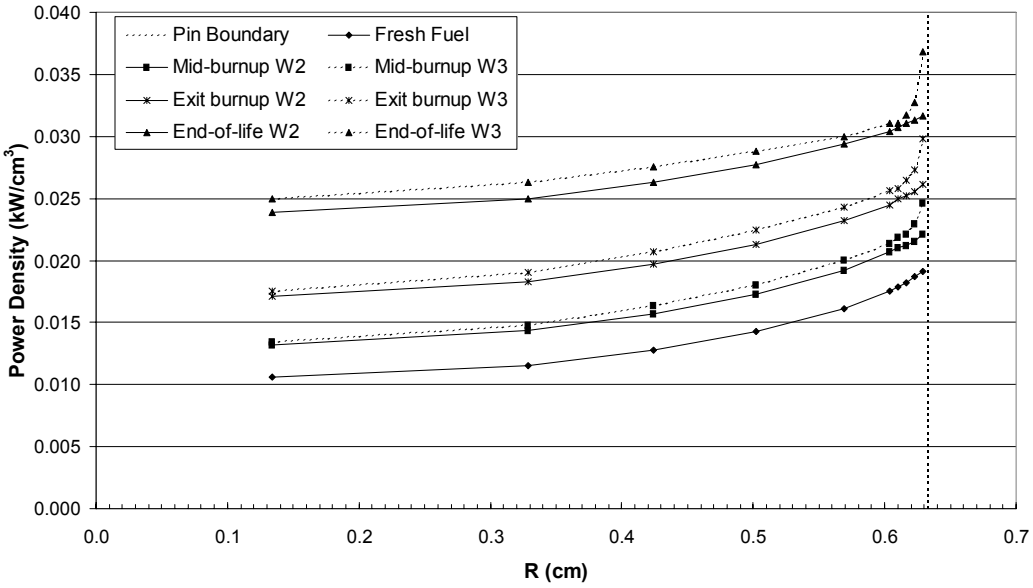

Photons produced near the edge have a greater probability to escape from the fuel than photons produced in the centre, which reduces the HPFPR.

The WIMS code associates an energy value with each fission, which includes all sources mentioned above. It does not treat heating from radiative captures explicitly, but a lattice-averaged heating value of 5.99 MeV (derived for NU fuel) is applied to every neutron that does not initiate a fission event (hence with each of ν-1 neutrons). This includes neutrons absorbed by the dysprosium although the Dy nucleus has an average capture gamma energy about 6.1 MeV. However, Dy capture gammas contribute only 0.5% to the total power output. Therefore the total heat was underestimated by (6.1-5.99)/6.1 x 0.5% = 0.009%.

5. Conclusions

The presence of the neutron absorber Dy, through its heat from capture (photon and ^{165}Dy beta energy), contributes 26% to the power in the central pin and 0.5% to the total power in the fuel, for fresh fuel. With irradiation, the dysprosium burns out, and for the central pin the fission

power increases while the dysprosium captures decrease. At the end-of-life, dysprosium captures contribute about 11% to the central pin heating.

There is a substantial percentage of the Dy-capture gamma heating deposited locally in the central element. Combined with gammas from the neighbouring elements, this results in a heating-power to fission-power ratio of about 1.53 (1.63 for the normalized HPFPR) for fresh fuel. With the burn-out of dysprosium, the fission power of the central pin increases, and the relative heating from Dy- capture photons and externally generated photons decreases; hence the decrease in the HPFPR in the central pin. The power-density distribution inside the central pin shows a peaking trend towards the edge.

It should be emphasized that the Dy does not release additional energy in the bundle. In the absence of Dy, neutrons would be absorbed elsewhere, causing a similar amount of energy to be released. However, a redistribution of the power does take place.

WIMS-AECL provides the fission power. To obtain the heating power, the fission power must be multiplied by the HPFPR. This ratio is 1.63 for the central pin at its maximum value for fresh fuel, and decreases to around 1.19 at end-of-life burnup. A comparison with the more advanced (but not yet IST-certified) WIMS version 3.02 shows very similar results, with slightly lower HPFPRs for the central element. The use of the IST code WIMS-AECL can be considered as more conservative.

Note that

1. The redistribution of power does not affect the distribution of the neutron flux in the lattice (apart from a higher order temperature-reactivity feed back). Hence, reactivity effects such as void reactivity are not affected by the re-distribution of power.
2. The total power, as obtained from WIMS is correct (apart from the small correction to the Dy capture gammas as mentioned in the previous section). This means that the overall reactor power is not affected, and that quantities such as the H-factors (average cell power divided by neutron flux) are still valid. Also the assignment of a burnup value to the bundle as a whole as well as to the individual elements is still valid, because the definition of burnup is based on the fission powers.
3. The total power, as calculated by WIMS for an LVRF bundle, remains the same (and correct), regardless of whether a full LVRF core is modelled or a mixed core of 37-element and LVRF bundles.

6. REFERENCES

1. M. LISKA and D. MCARTHUR, “Bruce Power New Fuel Project”, Proc. 8th Intl. Conf. on CANDU Fuel, Honey Harbour, Canada, September 21-24 (2003).
2. T.E. BOOTH et al. (The X-5 Monte Carlo Team), “MCNP – A General Monte Carlo N-Particle Transport Code Version 5”, Los Alamos National Laboratory, LA-UR-03-1987, April (2003).
3. J.D. IRISH and S.R. DOUGLAS, “Validation of WIMS-IST” Proc. 23rd Annual CNS Conf., Toronto, Canada, June 2-5 (2002); Version used was 2.5; libraries: dysprosium burnup chain included.